Original Article

Feasibility of *in vivo* magnetic resonance elastography of mesenteric adipose tissue in Crohn's disease

Laura J. Jensen[1]^, Florian N. Loch[2]^, Carsten Kamphues[3]^, Mehrgan Shahryari[1]^, Stephan R. Marticorena Garcia[1]^, Britta Siegmund[4]^, Carl Weidinger[4]^, Anja A. Kühl[5]^, Bernd Hamm[1]^, Jürgen Braun[6]^, Ingolf Sack[1]^, Patrick Asbach[1]^, Rolf Reiter[1,7]^

[1]Department of Radiology, Charité – Universitätsmedizin Berlin, Corporate Member of Freie Universität Berlin and Humboldt-Universität zu Berlin, Berlin, Germany; [2]Department of Surgery, Charité – Universitätsmedizin Berlin, Corporate Member of Freie Universität Berlin and Humboldt-Universität zu Berlin, Berlin, Germany; [3]Department of Surgery, Park-Klinik Weißensee, Berlin, Germany; [4]Department of Gastroenterology, Infectious Diseases and Rheumatology, Charité – Universitätsmedizin Berlin, Corporate Member of Freie Universität Berlin and Humboldt-Universität zu Berlin, Berlin, Germany; [5]iPATH.Berlin-Immunopathology for Experimental Models, Core Facility, Charité – Universitätsmedizin Berlin, Corporate Member of Freie Universität Berlin and Humboldt-Universität zu Berlin, Berlin, Germany; [6]Department of Medical Informatics, Charité – Universitätsmedizin Berlin, Corporate Member of Freie Universität Berlin and Humboldt-Universität zu Berlin, Berlin, Germany; [7]Berlin Institute of Health at Charité – Universitätsmedizin Berlin, BIH Biomedical Innovation Academy, BIH Charité Digital Clinician Scientist Program, Berlin, Germany

Contributions: (I) Conception and design: LJ Jensen, FN Loch, C Kamphues, SR Marticorena Garcia, B Siegmund, B Hamm, J Braun, I Sack, R Reiter; (II) Administrative support: B Siegmund, B Hamm, P Asbach, J Braun, I Sack; (III) Provision of study materials or patients: B Siegmund, C Weidinger, AA Kühl, FN Loch, C Kamphues; (IV) Collection and assembly of data: LJ Jensen, FN Loch, M Shahryari, B Siegmund, C Weidinger, AA Kühl, J Braun, I Sack, P Asbach, R Reiter; (V) Data analysis and interpretation: R Reiter; (VI) Manuscript writing: All authors; (VII) Final approval of manuscript: All authors.

Correspondence to: Laura J. Jensen, MD. Department of Radiology, Charité – Universitätsmedizin Berlin, Corporate Member of Freie Universität Berlin and Humboldt-Universität zu Berlin, Hindenburgdamm 30, 12203 Berlin, Germany. Email: laura-jacqueline.jensen@charite.de.

Background: Although there is growing evidence that functional involvement and structural changes of mesenteric adipose tissue (MAT) influence the course of Crohn's disease (CD), its viscoelastic properties remain elusive. Therefore, we aimed to investigate the viscoelastic properties of MAT in CD using magnetic resonance elastography (MRE), providing reference values for CD diagnosis.

Methods: In this prospective proof-of-concept study, 31 subjects (CD: n=11; healthy controls: n=20) were consecutively enrolled in a specialized care center for inflammatory bowel diseases (tertiary/quaternary care). Inclusion criteria for the CD patients were a clinically and endoscopically established diagnosis of CD based on the clinical record, absence of other concurrent bowel diseases, scheduled surgery for the following day, and age of at least 18 years. Diagnoses were confirmed by histological analysis of the resected bowel the day after MRE. Subjects were investigated using MRE at 1.5-T with frequencies of 40–70 Hz. To retrieve shear wave speed (SWS), volumes of interest (VOIs) in MAT were drawn adjacent to CD lesions (MAT_{CD}) and on the opposite side without adjacent bowel lesions in patients (MAT_{CD_Opp}) and controls (MAT_{CTRL}). The presented study is not registered in the clinical trial platform.

Results: A statistically significant decrease in mean SWS of 7% was found for MAT_{CD_Opp} *vs.* MAT_{CTRL} (0.76±0.05 *vs.* 0.82±0.04 m/s, P=0.012), whereas there was a nonsignificant trend with an 8% increase for

^ ORCID: Laura J. Jensen, 0000-0002-6436-5733; Florian N. Loch, 0000-0003-1513-8339; Carsten Kamphues, 0000-0002-5406-8540; Mehrgan Shahryari, 0000-0002-3981-1711; Stephan R. Marticorena Garcia, 0000-0003-3782-3003; Britta Siegmund, 0000-0002-0055-958X; Carl Weidinger, 0000-0002-9948-0088; Anja A. Kühl, 0000-0003-2293-5387; Bernd Hamm, 0000-0002-9141-027X; Jürgen Braun, 0000-0001-5183-7546; Ingolf Sack, 0000-0003-2460-1444; Patrick Asbach, 0000-0002-6885-3283; Rolf Reiter, 0000-0002-9741-6736.

MAT_{CD} *vs.* MAT_{CD_Opp} (0.82±0.07 *vs.* 0.76±0.05 m/s, P=0.098) and no difference for MAT_{CD} *vs.* MAT_{CTRL}. Preliminary area under the receiver operating characteristic curve (AUC) analysis showed diagnostic accuracy in detecting CD to be excellent for SWS of MAT_{CD_Opp} [AUC =0.82; 95% confidence interval (CI): 0.64–0.96] but poor for SWS of MAT_{CD} (AUC =0.52; 95% CI: 0.34–0.73).

Conclusions: This study demonstrates the feasibility of MRE of MAT and presents preliminary reference values for CD patients and healthy controls. Our results motivate further studies for the biophysical characterization of MAT in inflammatory bowel disease.

Keywords: Inflammatory bowel disease; Crohn's disease (CD); magnetic resonance imaging (MRI); magnetic resonance elastography (MRE); mesenteric adipose tissue (MAT)

Submitted Jan 08, 2023. Accepted for publication May 22, 2023. Published online Jun 28, 2023.
doi: 10.21037/qims-23-41
View this article at: https://dx.doi.org/10.21037/qims-23-41

Introduction

Crohn's disease (CD) is a severe condition with a growing incidence worldwide, with an incidence of over 6 per 100,000 person-years in broad parts of Western Europe and North America and an annual rise of up to 11% in newly industrialized countries (1). It is characterized by chronic recurrent inflammation, frequently followed by complications such as strictures, abscesses, and fistulas (1-3). The exact underlying pathology remains unclear.

In 1932, Crohn *et al.* first described hyperplasia of mesenteric adipose tissue (MAT) adjacent to intestinal inflammation (4). Corresponding indirect signs were described by Sellink *et al.* in 1974, who observed an increased inter-enteric spacing in abdominal radiography with oral contrast agent administration (5). The hyperplastic fat wrapping—also known as creeping fat—around the intestine is pathognomonic of CD and is thus not found in other inflammatory bowel diseases such as ulcerative colitis.

More recent studies indicate that beyond the morphological changes, structural and functional aspects of MAT influence progression, prognosis, and outcome in CD (6-9). Increased permeability of the bowel wall with bacterial translocation to the MAT is presumed to have an active role in the course of the disease (10-12). In contrast, MAT is also considered a potential secondary barrier around the inflamed intestine with localized anti-inflammatory function and a protective effect against a systemic inflammatory response. It can be distinguished histopathologically from healthy MAT by its altered extracellular matrix, distinctively small adipocytes, and a specific microenvironment defined by higher levels of adipokines and immune cell infiltration (8,13). All these new insights have led to the assumption of MAT as a distinct organ and a possible target for future therapies (14,15). Different adipocytokines secreted by visceral fat were considered potential therapeutic targets (15). For example, inhibitors of the adipocytokine visfatin, which is known to be elevated in CD, were investigated in phase I trials (15-19). Nevertheless, no approved therapeutic agent has yet been found to target MAT in CD (15).

Quantitative imaging techniques, among them magnetic resonance elastography (MRE), have recently been extended to the assessment of intestinal involvement in inflammatory bowel disease (20-22). MRE has emerged as a method for the quantitative mapping of biomechanical properties of different biological tissues (23). Several links between viscoelasticity and clinical endpoints have been identified. In a feasibility study on patients with inflammatory bowel disease compared to healthy volunteers, shear wave speed (SWS) representing stiffness of the bowel wall was significantly increased in patients with CD and ulcerative colitis (20). Avila *et al.* correlated the stiffness value to intestinal fibrosis in patients with CD, allowing predictions on the further clinical course based on the fibrosis score (21).

Imaging methods for direct visualization of what surgeons and pathologists describe as creeping fat are evolving, but the influence of its biomechanical signature remains elusive (24-26). We hypothesize that the development of creeping fat as a secondary barrier to CD-related inflammation leads to altered viscoelastic properties, which can be noninvasively measured by MRE.

Therefore, we conducted a study investigating the viscoelastic properties of MAT in CD patients and healthy subjects using *in vivo* MRE. We present this article in accordance with the STARD reporting checklist (27) (available at https://qims.amegroups.com/article/view/10.21037/qims-23-41/rc).

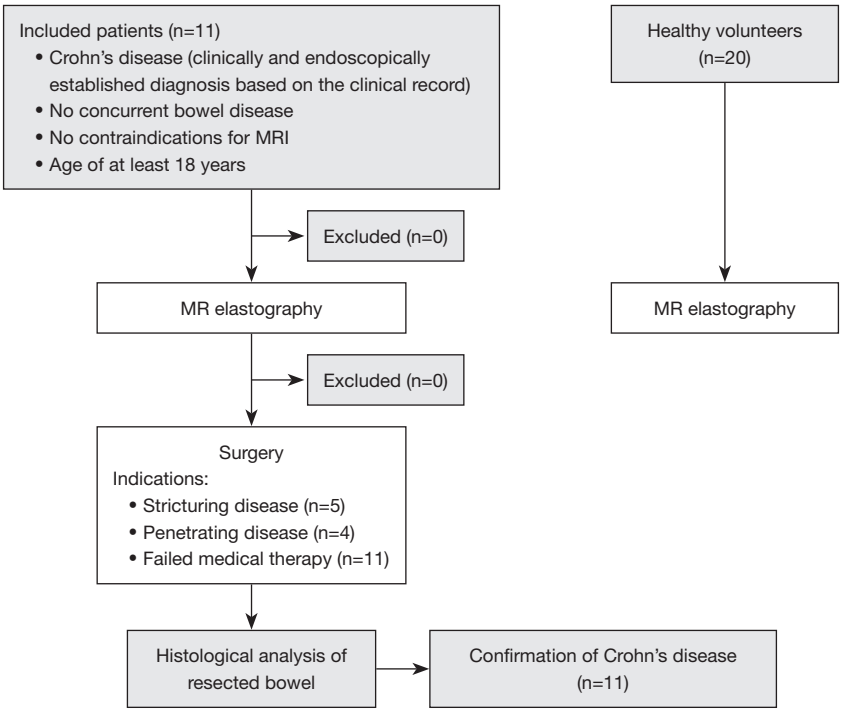

Figure 1 Flow diagram of the included patients. MR, magnetic resonance.

Methods

Subjects

The study was approved by the Institutional Review Board of Charité – Universitätsmedizin Berlin [protocol code (A1/075/17) and date of approval (5-11-2017)] and was conducted in accordance with the Declaration of Helsinki (as revised in 2013). Written informed consent was obtained from patients. Our institution is a specialized care center for inflammatory bowel diseases (tertiary/quaternary care). All elastography examinations were prospectively performed at a single institution from July 2019 through December 2020. Thirty-one subjects were consecutively included: CD patients (n=11) and healthy controls (n=20). Only patients with CD and no other inflammatory bowel diseases were included to focus on the elastography of creeping fat. For reasons of availability, more healthy individuals were examined. Inclusion criteria for patients were a clinically and endoscopically established diagnosis of CD based on the clinical record with clinically indicated surgery, absence of other concurrent bowel diseases, absence of general contraindications to MRI, and age of at least 18 years. Exclusion criteria were defined as increased peristalsis and fecal impaction. All patients met the eligibility criteria, and none were excluded. CD-related characteristics of patients are reported according to the Montreal classification, and diagnoses were confirmed by histological analysis of the resected bowel the day after MRE, which was used as standard of reference in all patients (28). The indication for surgery was stricture in five patients, penetrating disease in four patients, and failed medical therapy in all patients. *Figure 1* shows a flow diagram of the included patients. Of note, MRE data on the bowel wall have been reported before (20).

Tomoelastography

All examinations were performed on a 1.5-T MRI scanner (Magnetom Aera, Siemens Healthineers, Erlangen, Germany) using the spine-array coil in combination with an 18-channel body phased-array coil positioned on the patient's abdomen. Multifrequency MRE at 40, 50, 60, and 70 Hz with tomoelastography postprocessing was performed using 4 compressed-air drivers (20) and a single-shot spin-echo echo planar imaging (EPI) sequence (29,30). Further MRE scan parameters were: slices in axial orientation, 25; matrix, 100×66; resolution, 3×3×5 mm^3; TR, 3,070 ms, and TE, 50 ms; and total MRE acquisition

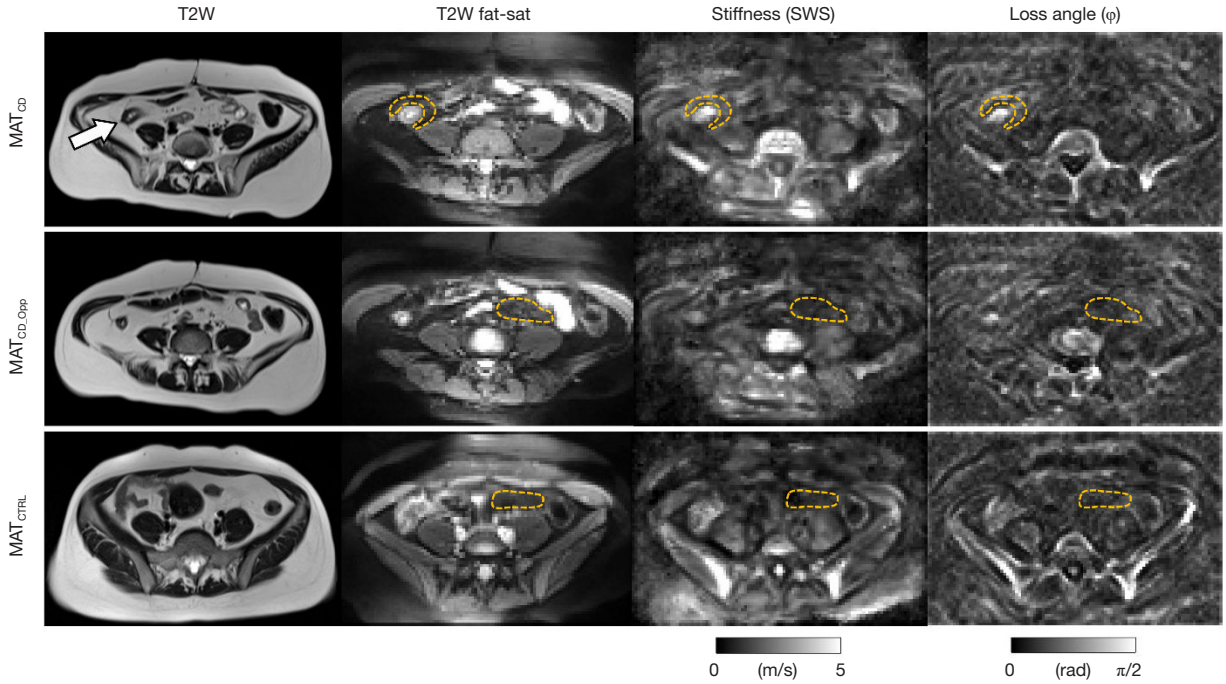

Figure 2 Cases. The yellow dotted lines show delineated VOIs in the MAT. The upper row shows a 41-year-old woman with CD with a SWS of 0.80±0.10 m/s and φ of 0.47±0.05 rad in the MAT_{CD}. The inflamed terminal ileum is indicated by an arrow. In the same patient, the middle row shows MAT_{CD_Opp} with a decreased SWS of 0.74±0.06 m/s and φ of 0.44±0.11 rad. The lower row depicts a 31-year-old healthy woman with an SWS of 0.84±0.15 m/s and φ of 0.58±0.21 rad (MAT_{CTRL}). T2W, T2-weighted; SWS, shear wave speed; φ, loss angle; MAT_{CD}, MAT with adjacent bowel lesion; MAT, mesenteric adipose tissue; MAT_{CD_Opp}, MAT without adjacent bowel lesion; MAT_{CTRL}, MAT of healthy controls; VOIs, volumes of interest.

time, 5:17 min. Subjects were breathing freely throughout MRE acquisition. No oral or intravenous contrast media or spasmolytic agents were administered. Quantitative maps of SWS (m/s) and loss angle of the complex modulus (φ, rad) representing stiffness and viscosity-related dispersion of stiffness over frequency, respectively, were generated using the publicly available tomoelastography processing pipeline (https://bioqic-apps.charite.de) (31-35). This pipeline offers a combination of two viscoelastic parameters that have been previously proposed for the investigation of many organs such as intestine (20), liver (36,37), kidney (38), parotid glands (39), and prostate (40). Reconstruction of SWS is based on the k-multifrequency dual elasto-visco (k-MDEV) inversion which represents a phase-gradient-based inversion with a Laplacian unwrapping method (35). Reconstruction of φ is based on the MDEV inversion which represents a direct inversion using a magnitude formulation and a gradient-based unwrapping method (41). Of note, φ ranges from 0 rad for pure solids to π/2 rad for pure fluids.

Volume of interest (VOI) analysis

VOIs were drawn on axial SWS maps using Matlab R2021b (MathWorks, Natick, MA, USA). Manually matched fat-saturated T2-weighted magnetic resonance images were used to locate MAT in healthy controls (MAT_{CTRL}) and bowel lesions in patients to place VOIs in adjacent MAT (MAT_{CD}). Additionally, VOIs in CD patients were also placed in MAT on the opposite side without adjacent bowel lesions (MAT_{CD_Opp}). VOIs were drawn independently by two readers (reader 1, LJJ: senior radiology resident with more than 5 years of experience; reader 2, RR: board-certified radiologist with over 10 years of experience in abdominal MRE). For the two readers, it was apparent on MRI scans whether participants were patients with CD or healthy subjects. Further clinical data were not available to the readers at the time of radiological assessment. In consensus, bowel lesions were defined as the most severely affected pathologically wall-thickened (>3 mm) intestinal loops. Moreover, VOIs were drawn on gluteal subcutaneous adipose tissue for inherent comparison. VOI placement is illustrated in *Figure 2*.

Table 1 Demographic baseline data of patients and healthy controls

Parameters	Patients (n=11)	Healthy controls (n=20)	P value
Gender (women/men), n (%)	6/5 (54.5/45.5)	10/10 (50.0/50.0)	–
Age (years), median [interquartile spacing]	38 [25]	31 [10]	0.47
BMI (kg/m^2), mean ± SD	21.8±3.4	22.0±2.6	0.84

BMI, body mass index; SD, standard deviation.

Table 2 Clinical details of CD patients according to the Montreal classification (29)

Montreal classification	Patients (n=11)
Age group at initial diagnosis	
A1, ≤16 years at diagnosis	1
A2, 17–40 years at diagnosis	8
A3, >40 years at diagnosis	2
Disease extent	
L1, terminal ileum	7
L2, colon	2
L3, ileocolon	2
L4, upper gastrointestinal tract	0
Disease behavior	
B1, nonstricturing, nonpenetrating	2
B2, stricturing	5
B3, penetrating	4
B3p, perianal penetrating	0
Perianal disease modifier	
No perianal disease	9
Perianal disease present	2
Medication history	
Corticosteroids	3
Infliximab	2
Adalimumab	2
Azathioprine	4

CD, Crohn's disease.

Statistical analysis

Continuous variables were described as mean ± standard deviation for data with normal distribution and as median with interquartile range (IQR) for data without normal distribution. Categorical variables were described as percentages. Group values of patients (MAT_{CD} and MAT_{CD_Opp}) and healthy controls (MAT_{CTRL}) were tested for differences using one-way analysis of variance (ANOVA) with Bonferroni-adjusted post-hoc analysis. Group values of gluteal subcutaneous adipose tissue between patients and healthy controls were compared with Welch's two sample *t*-test. Preliminary estimates of diagnostic accuracy in predicting CD were obtained by area under the receiver operating characteristic curve (AUC) analysis with a 95% confidence interval (CI). The Pearson correlation coefficient (r) was determined to assess the relationship between MRE parameters, age, body mass index (BMI), duration of disease, and C-reactive protein. All cases were re-evaluated to assess reproducibility by calculating intraclass correlation coefficients (ICCs) for interobserver agreement with 95% CI. Interobserver reliability was classified from poor to excellent (poor, <0.50; moderate, 0.50–0.75; good, 0.75–0.90; excellent, >0.90) (42). A P value <0.05 was considered to indicate statistical significance. R Studio (version 1.3.1093; R-Foundation, Vienna, Austria) was used for statistical analysis.

Results

MRE examinations were feasible in all 11 patients (median age: 38 years; IQR: 25 years; mean BMI: 21.8±3.4 kg/m^2; 6 women) and 20 healthy controls (median age: 31 years, IQR: 10 years; mean BMI: 22.0±2.6 kg/m^2; 10 women). An overview of demographic baseline data is shown in *Table 1*. Patients had a mean duration of CD of 150.0±111.4 months and a median C-reactive protein of 36.25 mg/L (IQR: 88.6 mg/L). Further CD-related clinical details of patients are listed in *Table 2*. *Figure 2* shows representative cases of a CD patient and healthy control. Median VOI size was 7.6 cm^3 (IQR: 6.9 cm^3).

Group values

As shown in *Figure 3*, a statistically significant decrease

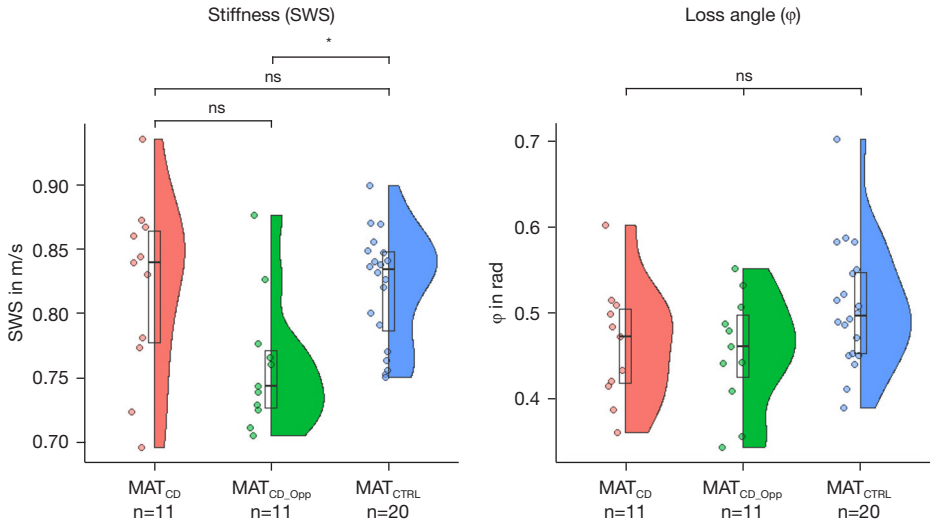

Figure 3 Box plots (displaying median, upper, and lower quartiles, and whiskers) combined with half-violin plots and experimental data points of stiffness and φ comparing MAT_{CD}, on the MAT_{CD_Opp}, and in MAT_{CTRL}. Statistically significant differences are indicated by an asterisk (*) for P<0.05; n.s., not significant. SWS, shear wave speed; φ, loss angle; MAT_{CD}, MAT with adjacent bowel lesion; MAT, mesenteric adipose tissue; MAT_{CD_Opp}, MAT without adjacent bowel lesion; MAT_{CTRL}, MAT of healthy controls.

in mean SWS of 7% was found for MAT_{CD_Opp} *vs.* MAT_{CTRL} (0.76±0.05 *vs.* 0.82±0.04 m/s, P=0.012), whereas a nonsignificant trend with an 8% increase in mean SWS was found for MAT_{CD} *vs.* MAT_{CD_Opp} (0.82±0.07 *vs.* 0.76±0.05 m/s, P>0.99) and no difference for MAT_{CD} *vs.* MAT_{CTRL} (0.82±0.07 *vs.* 0.82±0.04 m/s, P>0.99). For mean φ, no significant difference was found for any of these pairwise comparisons with P=0.179, 1.000, 0.342; respectively (MAT_{CD}: 0.46±0.07 rad; MAT_{CD_Opp}: 0.46±0.07 rad; MAT_{CTRL}: 0.82±0.04 rad). Moreover, no significant difference was found for subcutaneous adipose tissue between CD patients and healthy controls (SWS: 1.00±0.22 *vs.* 1.08±0.24 m/s, P=0.38; φ: 0.52±0.04 *vs.* 0.55±0.05 rad, P=0.09).

Correlation analysis

Pairwise Pearson correlation analysis of MRE parameters, age, BMI, duration of disease, and C-reactive protein did not reveal any significant correlations, except for a strong correlation between age and duration of disease (r=0.83, P=0.01) and a strong negative correlation between φ of MAT_{CD_Opp} and BMI (r=–0.79, P=0.004). *Table 3* provides an overview of all parameters of the correlation analysis. Of note, there was one data point missing for the C-reactive protein value and three data points for the duration of the disease because these patients were referred to our department of surgery from another hospital.

Diagnostic performance

Preliminary AUC analysis showed an excellent diagnostic accuracy of SWS of MAT_{CD_Opp} in detecting CD with an AUC =0.82 (95% CI: 0.64–0.96), whereas accuracy of SWS of MAT_{CD}, φ of MAT_{CD} and φ of MAT_{CD_Opp} was poor to moderate with an AUC =0.52, 0.67, 0.69 (95% CI: 0.34–0.73, 0.48–0.84, 0.51–0.85), respectively. Moreover, sensitivities, specificities, positive predictive values, and negative predictive values with optimal cut-offs using the Youden index are listed in *Table 4*. A cross-tabulation of SWS and φ results against the reference standard according to the AUC analysis is shown in *Table 5*.

Reproducibility

Interobserver agreement was good for MAT_{CD} with ICC =0.83 (95% CI: 0.39–0.95) for SWS and ICC =0.90 (95% CI: 0.63–0.97) for φ, good to excellent for MAT_{CD_Opp} with ICC =0.83 (95% CI: 0.37–0.95) for SWS and ICC =0.92 (95% CI: 0.70–0.98) for φ, and good for MAT_{CTRL} with ICC =0.84 (95% CI: 0.56–0.94) for SWS and ICC =0.90 (95% CI: 0.75–0.96) for φ. Moreover, agreement between the two readers for SWS and φ is shown in Bland-Altman plots in *Figure 4*.

Table 3 Correlation analysis with Pearson correlation coefficients r (upper triangle array) and corresponding P values (lower triangle array) for all demographic and imaging parameters of patients (n=11)

Categories	SWS of MAT_{CD}	φ of MAT_{CD}	SWS of MAT_{CD_Opp}	φ of MAT_{CD_Opp}	BMI	Age	Duration of disease	CRP
SWS of MAT_{CD}	–	0.38 (–0.28 to 0.80)	0.43 (–0.23 to 0.82)	0.21 (–0.45 to 0.72)	–0.03 (–0.62 to 0.58)	–0.22 (–0.72 to 0.44)	0.36 (–0.31 to 0.79)	–0.13 (–0.68 to 0.51)
φ of MAT_{CD}	0.25	–	0.43 (–0.23 to 0.82)	0.27 (–0.39 to 0.75)	–0.05 (–0.63 to 0.57)	0.15 (–0.49 to 0.69)	0.16 (–0.49 to 0.69)	0.27 (–0.39 to 0.75)
SWS of MAT_{CD_Opp}	0.19	0.19	–	0.49 (–0.16 to 0.84)	–0.28 (–0.75 to 0.38)	–0.43 (–0.82 to 0.23)	–0.26 (–0.74 to 0.40)	0.37 (–0.30 to 0.79)
φ of MAT_{CD_Opp}	0.54	0.42	0.13	–	–0.79* (–0.94 to –0.36)	–0.44 (–0.82 to 0.22)	–0.57 (–0.87 to 0.05)	0.21 (–0.45 to 0.72)
BMI	0.93	0.89	0.41	0.004*	–	0.35 (–0.32 to 0.79)	0.35 (–0.32 to 0.79)	–0.42 (–0.81 to 0.24)
Age	0.52	0.67	0.19	0.18	0.30	–	0.83* (0.46 to 0.95)	0.14 (–0.50 to 0.68)
Duration	0.38	0.71	0.53	0.14	0.40	0.01*	–	0.09 (–0.54 to 0.65)
CRP	0.72	0.44	0.29	0.56	0.22	0.70	0.86	–

Values in parentheses indicate 95% CI of r. *, significant correlation (P<0.05). SWS, shear wave speed; MAT_{CD}, MAT with adjacent bowel lesion; MAT, mesenteric adipose tissue; φ, loss angle; MAT_{CD_Opp}, MAT without adjacent bowel lesion; BMI, body mass index; CRP, C-reactive protein; CI, confidence interval.

Table 4 Diagnostic performance

Categories	Sn	Sp	NPV	PPV	AUC	Cut-off
SWS of MAT_{CD}	0.36 (0.13–0.63)	0.80 (0.65–0.95)	0.70 (0.54–0.85)	0.50 (0.20–0.80)	0.52 (0.34–0.73)	0.85 m/s
SWS of MAT_{CD_Opp}	0.75 (0.59–0.91)	0.82 (0.59–0.99)	0.64 (0.43–0.86)	0.88 (0.73–0.99)	0.82 (0.64–0.96)	0.78 m/s
φ of MAT_{CD}	0.90 (0.78–0.99)	0.46 (0.20–0.71)	0.71 (0.40–0.99)	0.75 (0.59–0.88)	0.67 (0.48–0.84)	0.43 rad
φ of MAT_{CD_Opp}	0.85 (0.71–0.99)	0.45 (0.20–0.71)	0.63 (0.33–0.99)	0.74 (0.57–0.89)	0.69 (0.51–0.85)	0.44 rad

Values in parentheses indicate 95% CI. Sn, sensitivity; Sp, specificity; NPV, negative predictive value; PPV, positive predictive value; AUC, area under the receiver operating characteristic curve (with an optimal cut-off using the Youden index); SWS, shear wave speed; MAT_{CD}, MAT with adjacent bowel lesion; MAT, mesenteric adipose tissue; φ, loss angle; MAT_{CD_Opp}, MAT without adjacent bowel lesion; CI, confidence interval.

Table 5 Comparison of the cut-off-based MRE diagnosis between the number of CD patients and healthy volunteers

Categories	MRE diagnosis, n (%)		Total, n
	Wrong	Right	
SWS of MAT_{CD}	11 (35.5)	20 (64.5)	31
SWS of MAT_{CD_Opp}	7 (22.6)	24 (77.4)	31
φ of MAT_{CD}	9 (29.0)	22 (71.0)	31
φ of MAT_{CD_Opp}	10 (32.3)	23 (74.2)	31

CD, Crohn's disease; MRE, magnetic resonance elastography; SWS, shear wave speed; MAT_{CD}, MAT with adjacent bowel lesion; MAT, mesenteric adipose tissue; φ, loss angle; MAT_{CD_Opp}, MAT on the opposite side without adjacent bowel lesions.

Discussion

In this proof-of-concept study, we demonstrate the feasibility of *in vivo* MRE of MAT and present preliminary reference values for CD patients and healthy controls. AUC results show diagnostic accuracy in detecting CD to be excellent for SWS of MAT_{CD_Opp} (AUC =0.82, 95% CI: 0.64–0.96) but poor for SWS of MAT_{CD} (AUC =0.52, 95% CI: 0.34–0.73). We found a statistically significant decrease in mean stiffness of 7% for MAT_{CD_Opp} compared to MAT_{CTRL}. This observation may suggest a general softening of MAT in CD with a trend toward 8% higher stiffness

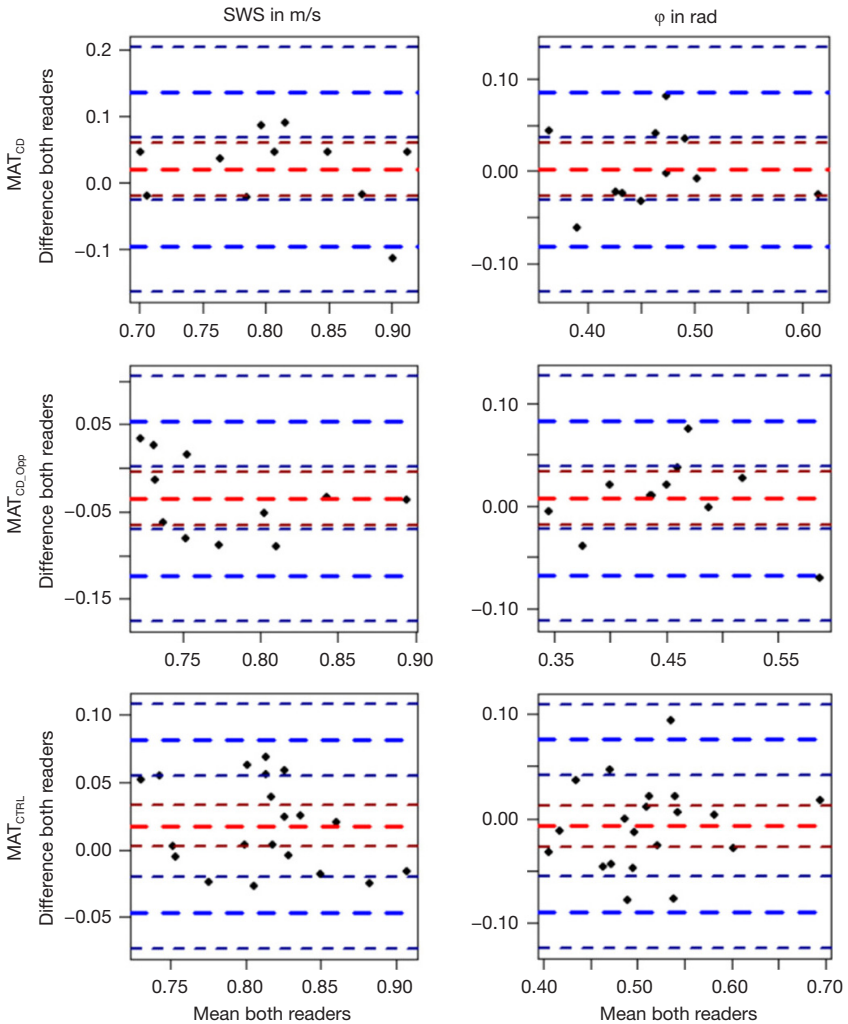

Figure 4 Bland-Altman plots show agreement between the two readers for SWS and φ. Single red bold dashed line = mean difference; paired blue bold dashed lines =95% limits of agreement (paired dark red and blue thin dashed lines = lower and upper limits of 95% CI). SWS, shear wave speed; φ, loss angle; MAT_{CD}, MAT with adjacent bowel lesion; MAT, mesenteric adipose tissue; MAT_{CD_Opp}, MAT without adjacent bowel lesion; MAT_{CTRL}, MAT of healthy controls; CI, confidence interval.

in areas of focal inflammatory bowel lesions (MAT_{CD}). This result could be attributed to the increased density of network elements by characteristically small adipocytes in CD, and enhanced leukocyte infiltration, which both contribute to the secondary barrier function of creeping fat. This biophysical signature may prevent bacterial translocation from the bowel walls with CD-related increased permeability, reducing the inflammatory response from systemic to localized. Moreover, the statistically significant negative correlation between φ of MAT_{CD_Opp} and BMI may be related to an increase in fluid-like properties of MAT with decreasing BMI in CD. Nevertheless, further studies with histopathological reference are needed to corroborate this preliminary hypothesis.

As the composition of extracellular matrix components of MAT is constantly changing during inflammation (13), a noninvasive imaging modality allowing the characterization of these changes would be a valuable new diagnostic tool. Despite the growing body of imaging studies aiming to quantify creeping fat in CD, little is known about its viscoelastic properties. For instance, van Schelt *et al.* examined seven patients with active CD and seven healthy volunteers using tomoelastography from 30–60 Hz and histopathological assessment in a subset of patients (43).

Preliminary results show no significant difference for mean SWS (CD: 0.80±0.21 *vs.* healthy: 0.67±0.07 m/s, P=0.18), whereas a significant increase was found for mean φ (CD: 0.58±0.15 *vs.* healthy: 0.45±0.08 rad, P=0.02). While our results are of the same order of magnitude, we found no significant group differences for φ. Possibly, this could be related to the use of mannitol solution as an oral contrast agent in patients but not in healthy controls and to the increased inflammation in active CD compared with our study with a rather fibrotic CD. We assumed a predominance of fibrotic over acute inflammatory changes in our CD patient collective as the indication for surgery was stricture in five patients and failed medical therapy in all patients, indicating a long-standing disease course. Desreumaux *et al.* observed a shift in the ratio of intra-abdominal fat to total body fat on MRI in CD patients compared to controls, indicating MAT hyperplasia in CD patients (26). As another approach to noninvasively quantify the presence of creeping fat, Li *et al.* developed a CT-based "mesenteric creeping fat index", which indirectly assesses creeping fat by using vascular findings as a surrogate (25). The proposed index allowed the authors to predict the extent of creeping fat in surgical specimens in a prospective study population with an AUC of 0.76 (25). Moreover, in a study using CT-enterography, Sakurai *et al.* found that mesenteric findings such as hypervascularity (comb sign) and enlarged mesenteric lymph nodes, rather than mural findings, were highly correlated with the endoscopically determined severity of mucosal ulcerations in CD (44).

Many MRI studies (12,45-49) and recently also a few MRE studies (20,21,30) assessed the bowel wall and not MAT. For instance, a recent MRE study conducted in a patient population overlapping with the present study showed significantly increased stiffness and loss angle of the bowel wall in inflammatory bowel disease (20). Compared to the present study, there was a strong correlation of φ between the bowel wall and adjacent MAT in CD patients (r=0.84, P=0.001), whereas no correlation was found for SWS (r=0.16, P=0.64). In another study, Avila *et al.* also reported increased stiffness in patients with CD as well as a link between advanced fibrosis on MRI and clinical events, e.g., surgical resection (21). Ultrasound-based elastography techniques have been used as diagnostic tools for the assessment of the bowel wall for more than two decades, however, without quantitative analysis of MAT (50).

Our study has limitations. First, we only investigated a small number of patients in this proof-of-concept study. Second, all CD patients and healthy controls have been reported previously (20). However, there is no overlap of MRE data as the earlier study focused on the bowel wall in inflammatory bowel disease. Third, intestinal adhesions and pathologically altered movements in CD might have influenced the comparison with healthy controls. Furthermore, no spasmolytic agents were administered to enable comparison with healthy controls in this explorative setting. Fourth, we have not performed a test-retest reproducibility assessment. However, we have found a good to excellent interreader agreement and another study investigating the prostate using the same tomoelastography setup demonstrated a good test-retest reproducibility (51). Fifth, the BMI distribution in our cohort reflects normal adult weight, which prevents an in-depth analysis of the interaction between BMI and MRE parameters. Nevertheless, in this exploratory proof-of-concept study, it is beneficial to avoid high variability in BMI as a confounding factor. Sixth, a biometric power analysis could not be performed in this exploratory proof-of-concept study as this is the first study to investigate the MRE-based viscoelastic properties of MAT in CD and no prior values were available. However, the results of this study provide a basis for planning future prospective studies. Finally, although all patients underwent surgery the day after the MRE scan and CD was histopathologically confirmed, there was no uniform or quantified account available for the extent of creeping fat or for the extent of intestinal inflammation and fibrosis. Nevertheless, we were able to measure MAT directly adjacent to pathological intestinal lesions. Still, other factors, such as mesenteric inflammation and fibrosis, might have had an influence. Future studies should take this into consideration to further improve the correlation of quantitative parameters. Using intraoperative ultrasound elastography or tabletop MRE of surgical specimens would allow a direct comparison of the mechanical properties of creeping fat with histopathology.

Conclusions

In this proof-of-concept study, we demonstrate the feasibility of *in vivo* MRE of MAT and present preliminary reference values for CD patients and healthy controls. Our results provide a basis for future study planning and motivate further studies for the biophysical characterization of MAT in CD in a bigger patient collective with histopathological scoring. Threshold values

of creeping fat would be desirable, possibly enabling predictions of early therapy response and the course of CD in clinical routine.

Acknowledgments

Preliminary results of this work were presented at the Annual Meeting of the International Society for Magnetic Resonance in Medicine in 2020 (Abstract #3336).

Funding: This study was funded by the Deutsche Forschungsgemeinschaft (DFG, German Research Foundation): SFB 1340/1 "Matrix in Vision" project number 372486779 (to BH, IS, PA, AAK, and BS), GRK 2260 BIOQIC (to IS), RE 4161/2-1 (to RR), and SFB-TR 241 "IEC in IBD" (to AAK, CW, and BS). This work was supported by BIH Digital Clinician Scientist Program funded by Charité – Universitätsmedizin Berlin, Berlin Institute of Health and the DFG (to RR).

Footnote

Reporting Checklist: The authors have completed the STARD reporting checklist. Available at https://qims.amegroups.com/article/view/10.21037/qims-23-41/rc

Conflicts of Interest: All authors have completed the ICMJE uniform disclosure form (available at https://qims.amegroups.com/article/view/10.21037/qims-23-41/coif). BH, IS, PA, AAK, and BS report that this study was funded by the Deutsche Forschungsgemeinschaft (DFG, German Research Foundation): SFB 1340/1 "Matrix in Vision" project number 372486779; IS reports that this study was funded by GRK 2260 BIOQIC; RR reports that this study was funded by RE 4161/2-1; AAK, CW, and BS report that this study was funded by SFB-TR 241 "IEC in IBD". RR is a participant of the BIH-Charité Digital Clinician Scientist Program funded by Charité – Universitätsmedizin Berlin, Berlin Institute of Health and the DFG. BS has received grant money from Pfizer, consultancy fees from Abbvie, Arena Pharma, Boehringer, BMS, Celgene, CT-Scout, Galapagos, Gilead, Janssen, Lilly, Pfizer, PredictImmune, PsiCro, and honoraria for lectures, presentations from Abbvie, CED Service GmbH, CHiesi, Galapagos, Falk Foundation, Forga Software, IBD passport, Janssen, Materia Prima, Pfizer, Lilly (all payments were made to Charité). BH is a grant recipient for the Department of Radiology from Abbott, AbbVie, Ablative Solutions, Accovion, Achogen Inc., Actelion Pharmaceuticals, ADIR, Aesculap, Agios Pharmaceuticals, Inc., AGO, Arbeitsgemeinschaft Industrieller Forschungsvereinigungen (AIF), Arbeitsgemeinschaft Internistische Onkologie (AIO), Aktionsbündnis Partnersicherheit e.V., Alexion Pharmaceuticals, Amgen, AO Foundation, Aravive, Arena Pharmaceuticals, ARMO Biosciences, Inc., Array Biopharma Inc., Art Photonics GmbH Berlin, ASAS, Ascelia Pharma AB, Ascendis, ASR Advanced Sleep Research, Astrellas, AstraZeneca, August Research OOF, Sofia, BG, BARD, Basiliea, Bayer Healthcare, Bayer Schering Pharma, Bayer Vital, BBraun, BerGenBioASA, Berlin-Brandenburger Centrum für Regenerative Therapie (BCRT), Berliner Krebsgesellschaft, Biontech Mainz, BioNTech SE, Biotronik, Bioven, BMBF, BMS, Boehring Ingelheimer, Boston Biomedical Inc., Boston Scientific Medizintechnik GmbH, BRACCO Group, Brahms GmbH, Brainsgate, Bistol-Myers Squibb, Calithera Biosciences UK, Cantargia AB, Medicon Village, Cascadian Therapeutics, Inc., Celgene, CELLACT Pharma, Celldex Therapeutics, Cellestia Biotech AG CH, CeloNova BioSciences, Charité Research Organization GmbH, Chiltern, Clovis Oncology, Inc., Covance, CRO Charité, CTI Ulm, CUBIST, CureVac AG, Tübingen, Curis, Daiichi Sankyo, Dartmouth College, Hanover, NH, USA, DC Devices, Inc. USA, Delcath Systems, Dermira Inc., Deutsche Krebshilfe, Deutsche Rheuma Liga, DZ-Deutsche Diabetes Forschungsgesellschaft e.V., Deutsches Zentrum für Luft- und Raumfahrt e.V., DFG, Dr. Falk Pharma GmbH, DSM Nutritional Products AG, Dt. Gesellschaft für Muskuloskelettale Radiologie, Dt. Stiftung für Herzforschung, Dynavax, Aisai Ltd., European Knowledge Centre, Mosquito Way, Hatfield, Eli Lilly and Company Ltd., EORTC, Episurf Medical, Epizyme, Inc., Essex Pharma, EU Programmes, European Society of Gastrointestinal and Abdominal Radiology, Euroscreen S.A., F20 Biotech GmbH, Ferring Pharmaceuticals A/S, Fibrex Medical Inc., Focused Ultrasound Surgery Foundation, Fraunhofer Gesellschaft, GALA Therapeutics, US, Galena Biopharma, Galmed Research and Development Ltd., Ganymed, GBG Forschungs GmbH, GE, Gentech. Inc., Genmab A/S, Genzyme Europe B.V., GETNE (Grupo Espanol de Tumores Neuroendocrinos), Gilead Sciences, Inc., Glaxo Smith Kline, Glycotype GmbH Berlin, Goethe Uni Frankfurt, Guerbet, Guidant Europe NV, Halozyme, Hans-Böckler-Stiftung, Hewlett Packard GmbH, Holaira Inc., Horizon Therapeutics Ireland, ICON (CRO), Idera Pharmaceuticals, Inc., Ignyta, Inc., Immunomedics Inc., Immunocore, Inari Medical Europe GmbH Basel, Incyte,

INC Research, Innate Pharma, InSightec Ltd., Inspiremd, InVentiv Health Clinical UK Ltd., Inventivhealth, IO Biotech ApS Copenhagen, IOMEDICO, IONIS, IPSEN Pharma, IQVIA ISA Therapeutics, Isis Pharmaceuticals Inc., ITM Solucin GmbH, Jansen-Cilag GmbH, Kantar Health GmbH (CRO), Kartos Therapeutics, Inc., Karyopharm Therapeutics, Inc., Kendle/MorphoSys AG, Kite Pharma, Kli Fo Berlin Mitte, Kura Oncology, Labcorb, La Roche, Land Berlin, Lilly GmbH, Lion Biotechnology, Lombard Medical, Loxo Oncology, Inc., LSK BioPartners, USA, Lundbeck GmbH, LUX Biosciences, LYSARC, MacroGenics, MagForce, MedImmune Inc., MedImmune Limited, Medpace, Medpace Germany GmbH (CRO), MedPass (CRO), Medtronic, Medtraveo GmbH, Merck, Merrimack Pharmaceuticals Inc., MeVis Medical Solutions AG, Millenium Pharmaceuticals Inc., Miltenyi Biomedicine GmbH, Bergisch Gladbach, miRagen Boukider, Mologen, Monika Kutzner Stiftung, MophoSys AG, MSD Sharp, Nektar Therapeutics, NeoVacs SA, Netzwerkverbund Radiologie, Neurocrine Biosciences Inc., US, Newlink Genetics Corporation, Nexus Oncology, NIH, NOGGO Berlin, Nord-Ostddeutsche Gesellschaft e.V., Novartis, Novocure, Nuvisan, Ockham oncology, Odonate Therapeutics San Diego, OHIRC Kanada, Oppilan Pharma Ltd., London, Orion Corporation Orion Pharma, OSE Immunotherapeutics, Parexel CRO Service, Pentixal Pharma GmbH Perceptive, Pfizer GmbH, PharmaCept GmbH, Pharma Mar, Pharmaceutical Reseach Associates GmbH (PRA), Pharmacyclics Inc., Philipps, Philogen s.p.a. Siena, Pliant Therapeutics San Francisco, PIQUR Therapeutics Ltd., Pluristem, PneuRX.Inc., Portola Pharmaceuticals, PPD (CRO), PRaint, Precision GmbH, Premier-Research, Priovant Therapeutics USA, Provectus Biopharmaceuticals, Inc., Psi-Cro, Pulmonx International Sarl, Quintiles GmbH, Radiobotics ApS, Regeneraon Pharmaceuticals Inc., Replimune, Respicardia, Rhythm Pharmaceuticals, Inc. Boston USA, Roche, Salix Pharmaceuticals Inc., Samsung, Sanofi, Sanofis-Aventis S.A., Sarepta Therapeutics, Cambridge, US, Saving Patient's Lives Medical B.V., Schumacher GmbH, Seagen, Seattle Genetics, Servier (CRO), SGS Life Science Sercives (CRO), Shape Memorial Midical Inc., USA, Shire Human Genetic Therapies, Siemens, Silena Therapeutics, SIRTEX Medical Europe GmbH, SOTIO Biotech, Boston, Spectranetics GmbH, Spectrum Pharmaceuticals, Stiftung Charite/BIH, St. Jude Medical, Stiftung Wolfgang Schulze, Syneos Health UK, Ltd., Symphogen, Taiho Oncology, Inc., Taiho Pharmaceutical Co., Target Pharma Solutions Inc., TauRx Therapeutics Ltd., Terumo Medical Corporation, Tesaro, Tetec-Ag, TEVA, Theorem, Theradex, Theravance, Threshold Pharmaceuticals Inc., TNS Healthcare GmbH, Toshiba, UCB Pharma, Ulrich GmbH Ulm, Uni Jena, Uni München, Uni Tübingen, Vaccibody A.S., VDI/VDE, Vertex Pharmaceuticals Incorporated, Viridian Therapeutics, US, Virtualscopis LLC, Winicker-Norimed, Wyeth Pharma, Xcovery Holding Company, and Zukunftsfond Berlin (TSB) outside the presented study. The other authors have no conflicts of interest to declare.

Ethical Statement: The authors are accountable for all aspects of the work in ensuring that questions related to the accuracy or integrity of any part of the work are appropriately investigated and resolved. The presented study is not registered in the clinical trial platform. The study was approved by the Institutional Review Board of Charité – Universitätsmedizin Berlin [protocol code (A1/075/17) and date of approval (5-11-2017)] and was conducted in accordance with the Declaration of Helsinki (as revised in 2013). Written informed consent was obtained from patients.

References

1. Ng SC, Shi HY, Hamidi N, Underwood FE, Tang W, Benchimol EI, Panaccione R, Ghosh S, Wu JCY, Chan FKL, Sung JJY, Kaplan GG. Worldwide incidence and prevalence of inflammatory bowel disease in the 21st century: a systematic review of population-based studies. Lancet 2017;390:2769-78.
2. Peyrin-Biroulet L, Loftus EV Jr, Colombel JF, Sandborn WJ. The natural history of adult Crohn's disease in population-based cohorts. Am J Gastroenterol 2010;105:289-97.
3. Torres J, Mehandru S, Colombel JF, Peyrin-Biroulet L. Crohn's disease. Lancet 2017;389:1741-55.
4. Crohn BB, Ginzburg L, Oppenheimer GD. Landmark

article Oct 15, 1932. Regional ileitis. A pathological and clinical entity. By Burril B. Crohn, Leon Ginzburg, and Gordon D. Oppenheimer. JAMA 1984;251:73-9.
5. Sellink JL. Radiologic examination of the small intestine by duodenal intubation. Acta Radiol Diagn (Stockh) 1974;15:318-32.
6. da Silva FAR, Pascoal LB, Dotti I, Setsuko Ayrizono ML, Aguilar D, Rodrigues BL, Arroyes M, Ferrer-Picon E, Milanski M, Velloso LA, Fagundes JJ, Salas A, Leal RF. Whole transcriptional analysis identifies markers of B, T and plasma cell signaling pathways in the mesenteric adipose tissue associated with Crohn's disease. J Transl Med 2020;18:44.
7. Siegmund B. Mesenteric fat in Crohn's disease: the hot spot of inflammation? Gut 2012;61:3-5.
8. Kredel L, Batra A, Siegmund B. Role of fat and adipokines in intestinal inflammation. Curr Opin Gastroenterol 2014;30:559-65.
9. Dowling L, Jakeman P, Norton C, Skelly MM, Yousuf H, Kiernan MG, Toomey M, Bowers S, Dunne SS, Coffey JC, Dunne CP. Adults with Crohn's disease exhibit elevated gynoid fat and reduced android fat irrespective of disease relapse or remission. Sci Rep 2021;11:19258.
10. Bischoff SC, Barbara G, Buurman W, Ockhuizen T, Schulzke JD, Serino M, Tilg H, Watson A, Wells JM. Intestinal permeability--a new target for disease prevention and therapy. BMC Gastroenterol 2014;14:189.
11. Camilleri M. Leaky gut: mechanisms, measurement and clinical implications in humans. Gut 2019;68:1516-26.
12. Scott RA, Williams HG, Hoad CL, Alyami A, Ortori CA, Grove JI, Marciani L, Moran GW, Spiller RC, Menys A, Aithal GP, Gowland PA. MR Measures of Small Bowel Wall T2 Are Associated With Increased Permeability. J Magn Reson Imaging 2021;53:1422-31.
13. Golusda L, Kühl AA, Siegmund B, Paclik D. Extracellular Matrix Components as Diagnostic Tools in Inflammatory Bowel Disease. Biology (Basel) 2021;10:1024.
14. Rivera ED, Coffey JC, Walsh D, Ehrenpreis ED. The Mesentery, Systemic Inflammation, and Crohn's Disease. Inflamm Bowel Dis 2019;25:226-34.
15. Eder P, Adler M, Dobrowolska A, Kamhieh-Milz J, Witowski J. The Role of Adipose Tissue in the Pathogenesis and Therapeutic Outcomes of Inflammatory Bowel Disease. Cells 2019.
16. Fukuhara A, Matsuda M, Nishizawa M, Segawa K, Tanaka M, Kishimoto K, et al. Visfatin: a protein secreted by visceral fat that mimics the effects of insulin. Science 2005;307:426-30.
17. Gerner RR, Klepsch V, Macheiner S, Arnhard K, Adolph TE, Grander C, Wieser V, Pfister A, Moser P, Hermann-Kleiter N, Baier G, Oberacher H, Tilg H, Moschen AR. NAD metabolism fuels human and mouse intestinal inflammation. Gut 2018;67:1813-23.
18. Starr AE, Deeke SA, Ning Z, Chiang CK, Zhang X, Mottawea W, Singleton R, Benchimol EI, Wen M, Mack DR, Stintzi A, Figeys D. Proteomic analysis of ascending colon biopsies from a paediatric inflammatory bowel disease inception cohort identifies protein biomarkers that differentiate Crohn's disease from UC. Gut 2017;66:1573-83.
19. Moschen AR, Kaser A, Enrich B, Mosheimer B, Theurl M, Niederegger H, Tilg H. Visfatin, an adipocytokine with proinflammatory and immunomodulating properties. J Immunol 2007;178:1748-58.
20. Reiter R, Loch FN, Kamphues C, Bayerl C, Marticorena Garcia SR, Siegmund B, Kühl AA, Hamm B, Braun J, Sack I, Asbach P. Feasibility of Intestinal MR Elastography in Inflammatory Bowel Disease. J Magn Reson Imaging 2022;55:815-22.
21. Avila F, Caron B, Hossu G, Ambarki K, Kannengiesser S, Odille F, Felblinger J, Danese S, Choukour M, Laurent V, Peyrin-Biroulet L. Magnetic Resonance Elastography for Assessing Fibrosis in Patients with Crohn's Disease: A Pilot Study. Dig Dis Sci 2022;67:4518-24.
22. Li XH, Mao R, Huang SY, Sun CH, Cao QH, Fang ZN, Zhang ZW, Huang L, Lin JJ, Chen YJ, Rimola J, Rieder F, Chen MH, Feng ST, Li ZP. Characterization of Degree of Intestinal Fibrosis in Patients with Crohn Disease by Using Magnetization Transfer MR Imaging. Radiology 2018;287:494-503.
23. Li Y, Gao Q, Chen N, Zhang Y, Wang J, Li C, He X, Jiao Y, Zhang Z. Clinical studies of magnetic resonance elastography from 1995 to 2021: Scientometric and visualization analysis based on CiteSpace. Quant Imaging Med Surg 2022;12:5080-100.
24. Mao R, Kurada S, Gordon IO, Baker ME, Gandhi N, McDonald C, Coffey JC, Rieder F. The Mesenteric Fat and Intestinal Muscle Interface: Creeping Fat Influencing Stricture Formation in Crohn's Disease. Inflamm Bowel Dis 2019;25:421-6.
25. Li XH, Feng ST, Cao QH, Coffey JC, Baker ME, Huang L, Fang ZN, Qiu Y, Lu BL, Chen ZH, Li Y, Bettenworth D, Iacucci M, Sun CH, Ghosh S, Rieder F, Chen MH, Li ZP, Mao R. Degree of Creeping Fat Assessed by Computed Tomography Enterography is Associated with Intestinal Fibrotic Stricture in Patients with Crohn's Disease: A

Potentially Novel Mesenteric Creeping Fat Index. J Crohns Colitis 2021;15:1161-73.
26. Desreumaux P, Ernst O, Geboes K, Gambiez L, Berrebi D, Müller-Alouf H, Hafraoui S, Emilie D, Ectors N, Peuchmaur M, Cortot A, Capron M, Auwerx J, Colombel JF. Inflammatory alterations in mesenteric adipose tissue in Crohn's disease. Gastroenterology 1999;117:73-81.
27. Bossuyt PM, Reitsma JB, Bruns DE, Gatsonis CA, Glasziou PP, Irwig L, Lijmer JG, Moher D, Rennie D, de Vet HC, Kressel HY, Rifai N, Golub RM, Altman DG, Hooft L, Korevaar DA, Cohen JF; STARD Group. STARD 2015: An Updated List of Essential Items for Reporting Diagnostic Accuracy Studies. Radiology 2015;277:826-32.
28. Silverberg MS, Satsangi J, Ahmad T, Arnott ID, Bernstein CN, Brant SR, et al. Toward an integrated clinical, molecular and serological classification of inflammatory bowel disease: report of a Working Party of the 2005 Montreal World Congress of Gastroenterology. Can J Gastroenterol 2005;19 Suppl A:5A-36A.
29. Dittmann F, Hirsch S, Tzschätzsch H, Guo J, Braun J, Sack I. In vivo wideband multifrequency MR elastography of the human brain and liver. Magn Reson Med 2016;76:1116-26.
30. Marticorena Garcia SR, Hamm B, Sack I. Tomoelastography for non-invasive detection and treatment monitoring in acute appendicitis. BMJ Case Rep 2019.
31. Streitberger KJ, Lilaj L, Schrank F, Braun J, Hoffmann KT, Reiss-Zimmermann M, Käs JA, Sack I. How tissue fluidity influences brain tumor progression. Proc Natl Acad Sci U S A 2020;117:128-34.
32. Hudert CA, Tzschätzsch H, Rudolph B, Bläker H, Loddenkemper C, Müller HP, Henning S, Bufler P, Hamm B, Braun J, Holzhütter HG, Wiegand S, Sack I, Guo J. Tomoelastography for the Evaluation of Pediatric Nonalcoholic Fatty Liver Disease. Invest Radiol 2019;54:198-203.
33. Guo J, Bertalan G, Meierhofer D, Klein C, Schreyer S, Steiner B, Wang S, Vieira da Silva R, Infante-Duarte C, Koch S, Boehm-Sturm P, Braun J, Sack I. Brain maturation is associated with increasing tissue stiffness and decreasing tissue fluidity. Acta Biomater 2019;99:433-42.
34. Shahryari M, Tzschätzsch H, Guo J, Marticorena Garcia SR, Böning G, Fehrenbach U, Stencel L, Asbach P, Hamm B, Käs JA, Braun J, Denecke T, Sack I. Tomoelastography Distinguishes Noninvasively between Benign and Malignant Liver Lesions. Cancer Res 2019;79:5704-10.
35. Tzschätzsch H, Guo J, Dittmann F, Hirsch S, Barnhill E, Jöhrens K, Braun J, Sack I. Tomoelastography by multifrequency wave number recovery from time-harmonic propagating shear waves. Med Image Anal 2016;30:1-10.
36. Reiter R, Tzschätzsch H, Schwahofer F, Haas M, Bayerl C, Muche M, Klatt D, Majumdar S, Uyanik M, Hamm B, Braun J, Sack I, Asbach P. Diagnostic performance of tomoelastography of the liver and spleen for staging hepatic fibrosis. Eur Radiol 2020;30:1719-29.
37. Reiter R, Shahryari M, Tzschätzsch H, Haas M, Bayerl C, Siegmund B, Hamm B, Asbach P, Braun J, Sack I. Influence of fibrosis progression on the viscous properties of in vivo liver tissue elucidated by shear wave dispersion in multifrequency MR elastography. J Mech Behav Biomed Mater 2021;121:104645.
38. Marticorena Garcia SR, Grossmann M, Bruns A, Dürr M, Tzschätzsch H, Hamm B, Braun J, Sack I, Guo J. Tomoelastography Paired With T2* Magnetic Resonance Imaging Detects Lupus Nephritis With Normal Renal Function. Invest Radiol 2019;54:89-97.
39. Elsholtz FHJ, Reiter R, Marticorena Garcia SR, Braun J, Sack I, Hamm B, Schaafs LA. Multifrequency magnetic resonance elastography-based tomoelastography of the parotid glands-feasibility and reference values. Dentomaxillofac Radiol 2022;51:20210337.
40. Asbach P, Ro SR, Aldoj N, Snellings J, Reiter R, Lenk J, Köhlitz T, Haas M, Guo J, Hamm B, Braun J, Sack I. In Vivo Quantification of Water Diffusion, Stiffness, and Tissue Fluidity in Benign Prostatic Hyperplasia and Prostate Cancer. Invest Radiol 2020;55:524-30.
41. Papazoglou S, Hirsch S, Braun J, Sack I. Multifrequency inversion in magnetic resonance elastography. Phys Med Biol 2012;57:2329-46.
42. Koo TK, Li MY. A Guideline of Selecting and Reporting Intraclass Correlation Coefficients for Reliability Research. J Chiropr Med 2016;15:155-63.
43. van Schelt A, Beek K, Wassenaar NPM, Schrauben EM, Runge JH, Nederveen AJ, Stoker J. MR Elastography of the Affected Mesenteric Fat in Active Crohn's Disease: A Feasibility Study. Proc Intl Soc Mag Reson Med 2022;16:3984.
44. Sakurai T, Katsuno T, Saito K, Yoshihama S, Nakagawa T, Koseki H, Taida T, Ishigami H, Okimoto KI, Maruoka D, Matsumura T, Arai M, Yokosuka O. Mesenteric findings of CT enterography are well correlated with the endoscopic severity of Crohn's disease. Eur J Radiol 2017;89:242-8.
45. Chang HC, Chen G, Chung HW, Wu PY, Liang L, Juan CJ, Liu YJ, Tse MD, Chan A, Zhang S, Chiu KW.

Multi-shot Diffusion-Weighted MRI With Multiplexed Sensitivity Encoding (MUSE) in the Assessment of Active Inflammation in Crohn's Disease. J Magn Reson Imaging 2022;55:126-37.
46. Zhang TT, Chang WC, Wang ZJ, Sun DC, Ohliger MA, Yeh BM. Bowel Wall Visualization Using MR Enterography in Relationship to Bowel Lumen Contents and Patient Demographics. J Magn Reson Imaging 2021;54:728-36.
47. Cruz-Romero C, Guo A, Bradley WF, Vicentini JRT, Yajnik V, Gee MS. Novel Associations Between Genome-Wide Single Nucleotide Polymorphisms and MR Enterography Features in Crohn's Disease Patients. J Magn Reson Imaging 2021;53:132-8.
48. Loch FN, Kamphues C, Beyer K, Klauschen F, Schineis C, Weixler B, Lauscher JC, Dorenbeck M, Bayerl C, Reiter R. Diagnostic Accuracy of Magnetic Resonance Enterography for the Evaluation of Active and Fibrotic Inflammation in Crohn's Disease. Front Surg 2022;9:872596.
49. Cakmakci E, Erturk SM, Cakmakci S, Bayram A, Tokgoz S, Caliskan KC, Celebi I. Comparison of the results of computerized tomographic and diffusion-weighted magnetic resonance imaging techniques in inflammatory bowel diseases. Quant Imaging Med Surg 2013;3:327-33.
50. Branchi F, Caprioli F, Orlando S, Conte D, Fraquelli M. Non-invasive evaluation of intestinal disorders: The role of elastographic techniques. World J Gastroenterol 2017;23:2832-40.
51. Dittmann F, Reiter R, Guo J, Haas M, Asbach P, Fischer T, Braun J, Sack I. Tomoelastography of the prostate using multifrequency MR elastography and externally placed pressurized-air drivers. Magn Reson Med 2018;79:1325-33.

Cite this article as: Jensen LJ, Loch FN, Kamphues C, Shahryari M, Marticorena Garcia SR, Siegmund B, Weidinger C, Kühl AA, Hamm B, Braun J, Sack I, Asbach P, Reiter R. Feasibility of *in vivo* magnetic resonance elastography of mesenteric adipose tissue in Crohn's disease. Quant Imaging Med Surg 2023;13(8):4792-4805. doi: 10.21037/qims-23-41

